

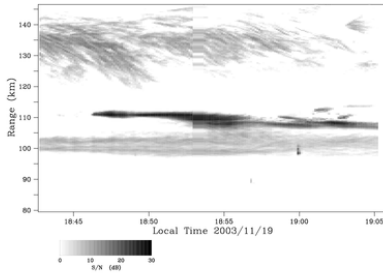
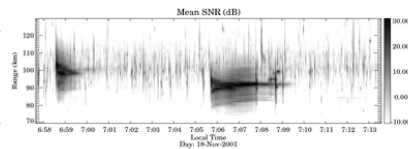
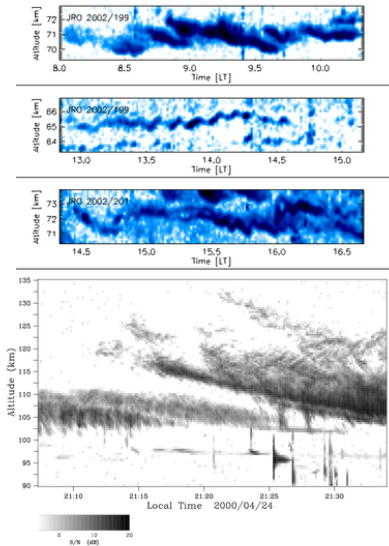
Equatorial Aeronomy

(<http://landau.geo.cornell.edu/papers/aeronomy.pdf>)

D. L. Hysell, Cornell University, September, 2014

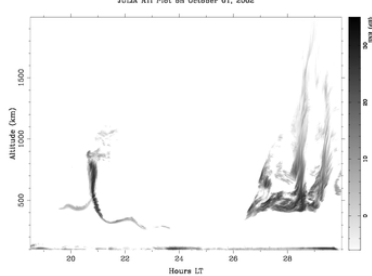
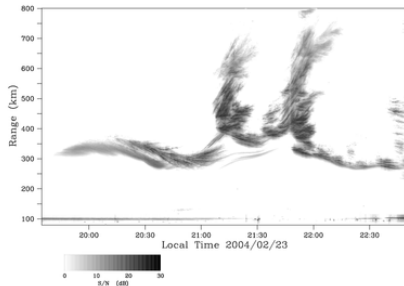
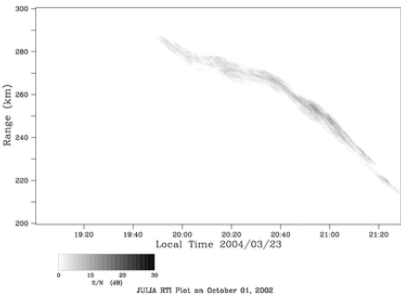
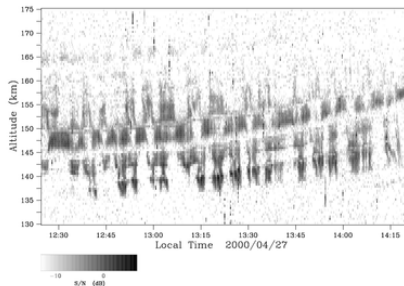


equatorial phenomena



movie

more examples



- survey of unique equatorial phenomena
- the geomagnetic field
- ionospheric electrodynamics
- dynamo theory
- prereversal enhancement, plasma shear; evening vortex
- equatorial E region, electrojet
- equatorial spread F
- topside, energetic electrons

dipole magnetic field

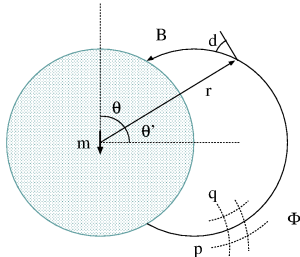
$$\phi_m = -\frac{\mathbf{m} \cdot \mathbf{r}}{r^3} = -\frac{\cos \theta}{r^2}$$

$$\mathbf{B} = -\nabla \phi_m = -\frac{2m \cos \theta}{r^3} \hat{r} - \frac{m \sin \theta}{r^3} \hat{\theta} = -\frac{3\hat{r}(\mathbf{m} \cdot \hat{r}) - \mathbf{m}}{r^3}$$

$$B = \frac{m}{r^3} (1 + 3 \cos^2 \theta)^{1/2}$$

$$\tan d = \frac{B_r}{B_\theta} = 2 \tan \theta'$$

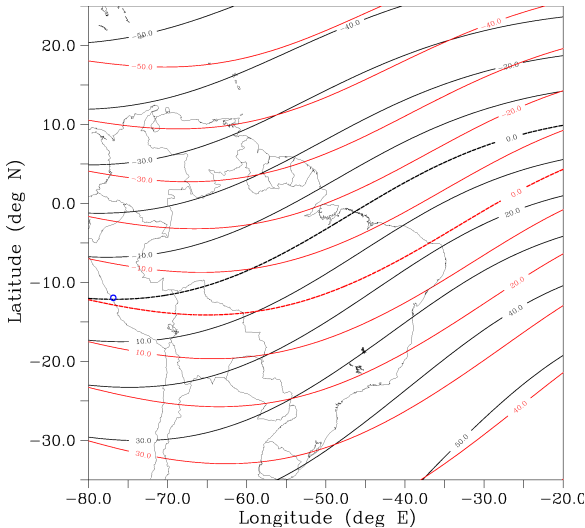
$$r = LR_e \sin^2 \theta \quad (p = r / \sin^2 \theta, q = \cos \theta / r^2, \Phi)$$



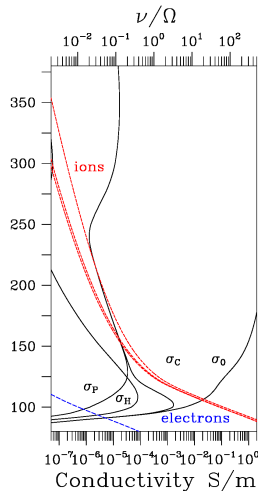
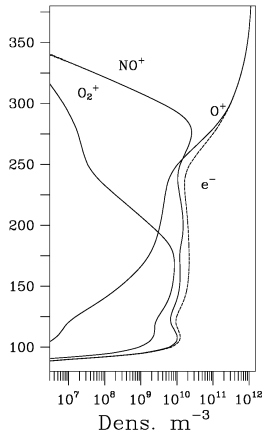
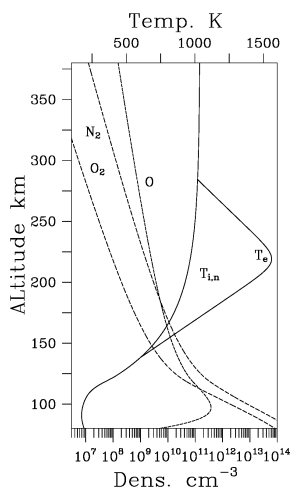
$$h_p = \sin^3 \theta / \delta, h_q = r^3 / \delta, h_\Phi = r \sin \theta$$

$$\delta = \sqrt{1 + 3 \cos^2 \theta}$$

non-dipole contribution



equatorial zone, twilight, moderate solar flux



low-frequency equilibrium dynamics; force balance

$$0 \approx q_s (\mathbf{E} + \mathbf{v}_s \times \mathbf{B}) - K_B T \nabla n_s / n_s - \sum_n \nu_{sn} m_s (\mathbf{v}_s - \mathbf{u}) + m_s \mathbf{g}$$
$$+ \dots$$

$$\mathbf{v}_s - \mathbf{u} = \mu_s \cdot (\mathbf{E} + \mathbf{u} \times \mathbf{B}) - \mathbf{D}_s \cdot \nabla n_s / n_s + \mathbf{T}_s \cdot \mathbf{g}$$

$$\mathbf{v}_{s\perp} \approx \begin{cases} \frac{\mathbf{E} \times \mathbf{B}}{B^2} & \nu_{sn} \ll |\Omega_s| \\ \mathbf{u}_\perp & \nu_{sn} \gg |\Omega_s| \end{cases}$$

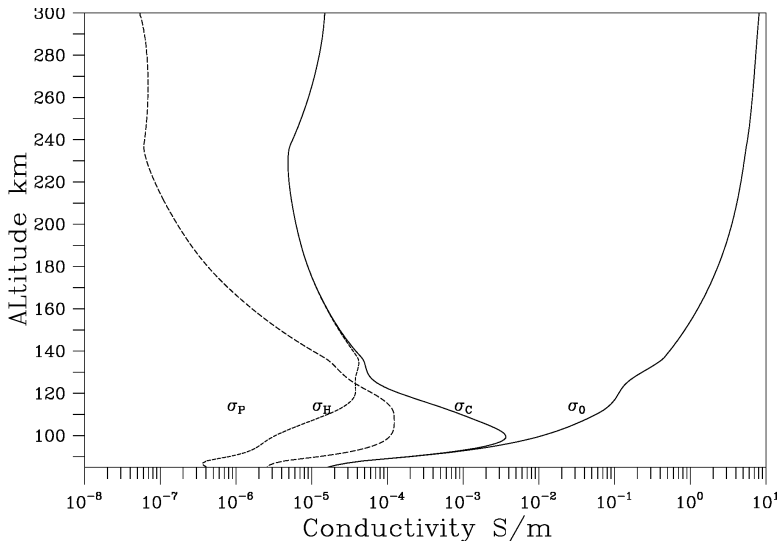
$$\begin{aligned} \mathbf{J} &\equiv \sum_s (q_s n_s \mathbf{v}_s) \\ &= \sigma \cdot (\mathbf{E} + \mathbf{u} \times \mathbf{B}) - \sum_s q_s \mathbf{D}_s \cdot \nabla n_s + \boldsymbol{\Xi} \cdot \mathbf{g} \end{aligned}$$

low-frequency conductivity (anisotropic)

$$\begin{aligned}\mathbf{J}_{\text{cond}} &= \begin{pmatrix} \sigma_P & \sigma_H \\ -\sigma_H & \sigma_P \\ & \sigma_o \end{pmatrix} \cdot \underbrace{(\mathbf{E} + \mathbf{u} \times \mathbf{B})}_{\mathbf{E}'} \\ &= \sigma_P (\mathbf{E}_\perp + \mathbf{u} \times \mathbf{B}) \\ &\quad + \sigma_H \hat{\mathbf{b}} \times (\mathbf{E}_\perp + \mathbf{u} \times \mathbf{B}) + \sigma_o \mathbf{E}_\parallel\end{aligned}$$

$$\begin{aligned}\sigma_P &= e^2 \sum_j \frac{n_j \nu_j}{m_j(\nu_j^2 + \Omega_j^2)} \\ \sigma_H &= e^2 \sum_j \frac{-n_j \Omega_j}{m_j(\nu_j^2 + \Omega_j^2)} \\ \sigma_o &= e^2 \sum_j \frac{n_j}{m_j \nu_j}\end{aligned}$$

conductivity profiles (twilight)



but what is \mathbf{E} ?: quasineutrality, polarization

$$\begin{aligned}\mathbf{J} &\equiv \sum_s (q_s n_s \mathbf{v}_s) \\ &= \sigma \cdot (\mathbf{E} + \mathbf{u} \times \mathbf{B}) - \sum_s q_s \mathbf{D}_s \cdot \nabla n_s + \boldsymbol{\Xi} \cdot \mathbf{g}\end{aligned}$$

statement of charge neutrality in a plasma:

$$\boxed{\nabla \cdot \mathbf{J} = 0}$$

polarization electric field:

$$\mathbf{E} \rightarrow \mathbf{E}_o - \nabla \phi$$

$$\nabla \cdot (\sigma \cdot \nabla \phi) = \nabla \cdot \left[\sigma \cdot (\mathbf{E}_o + \mathbf{u} \times \mathbf{B}) - \sum_s q_s \mathbf{D}_s \cdot \nabla n_s + \boldsymbol{\Xi} \cdot \mathbf{g} \right]$$

- conductivity anisotropic
- parallel electric fields small
- magnetic field lines act like equipotentials
- electric fields from induced dipole moments arise to preserve charge neutrality in presence of inhomogeneity
- local dynamics associated largely with these polarization electric fields
- polarization fields, in turn, influenced by numerous drivers (local and global)
- absent field-aligned currents, transverse (to B) currents flow along conductivity isocontours

dynamo theory (p, q, Φ) coordinate system

$$0 = \nabla \cdot \mathbf{J} \propto \frac{\partial}{\partial q} (h_p h_\phi J_q) + \frac{\partial}{\partial p} \left(h_q h_\phi \sigma_p \left\{ u_\phi B - \frac{1}{h_p} \frac{\partial \phi}{\partial p} \right\} \right)$$

integrate along \mathbf{B} between E -region conjugate points

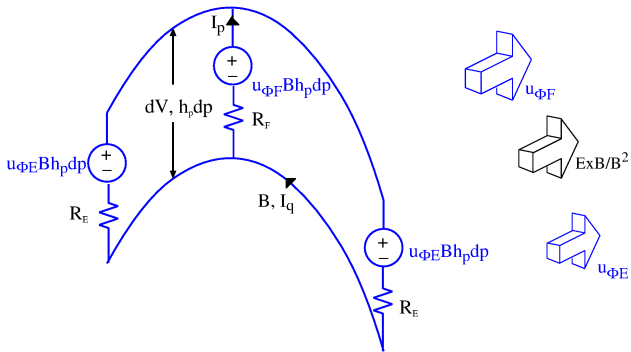
$$0 = \cancel{h_p h_\phi J_q|_E^F} + \underbrace{\int_{E-F-E} dq \frac{\partial}{\partial p} \left(h_q h_\phi \sigma_p \left\{ u_\phi B - \frac{1}{h_p} \frac{\partial \phi}{\partial p} \right\} \right)}_{\leftarrow}$$

$$\int_{E+E} dq h_q h_\phi \sigma_p u_\phi B + \int_F dq h_q h_\phi \sigma_p u_\phi B = \int_{E+F+E} dq \frac{h_q h_\phi}{h_p} \sigma_p \underbrace{\frac{\partial \phi}{\partial p}}_{\leftarrow}$$

$$\int dq h_{q\circ} h_\phi \sigma_p u_\phi B_\circ + \int dq h_{q\circ} h_\phi \sigma_p u_\phi B_\circ = \frac{1}{h_{p\circ}} \frac{\partial \phi}{\partial p_\circ} \int dq h_q h_\phi \frac{h_{p\circ}}{h_p} \sigma_p$$

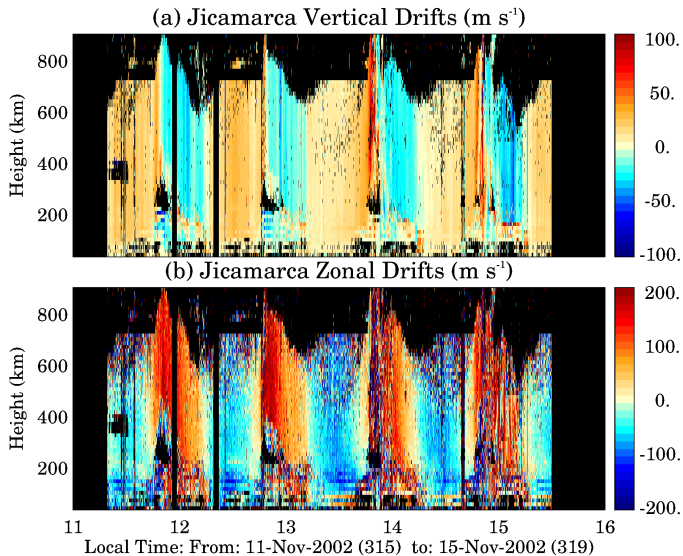
$\Sigma_{pE} u_{\phi E} B_\circ + \Sigma_{pF} u_{\phi F} B_\circ = -E_{p\circ} \Sigma_p$

circuit analogy

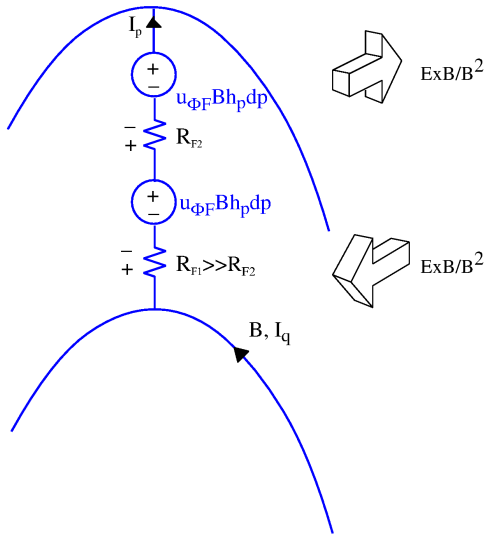


$$dV = \frac{u_{\Phi F} B h_p dp / R_F + u_{\Phi E} B h_p dp / R_E}{1/R_F + 1/R_E}$$

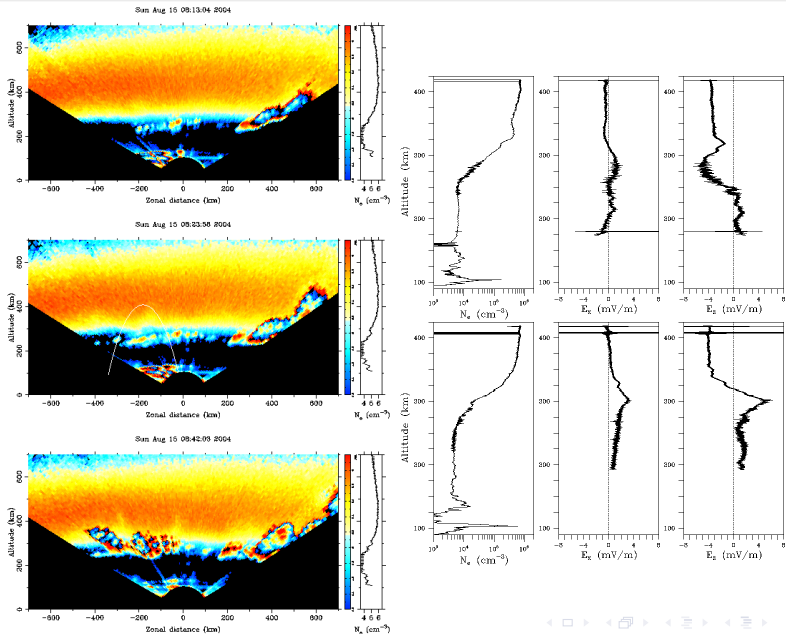
zonal drifts, super-rotation



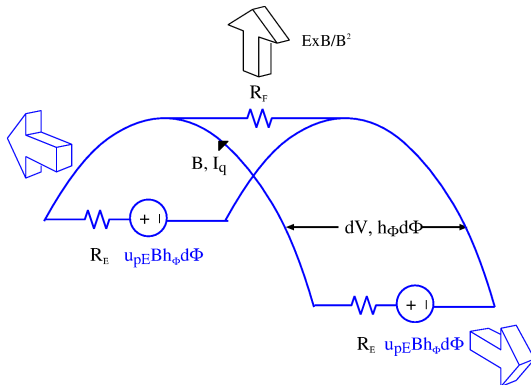
shear flow



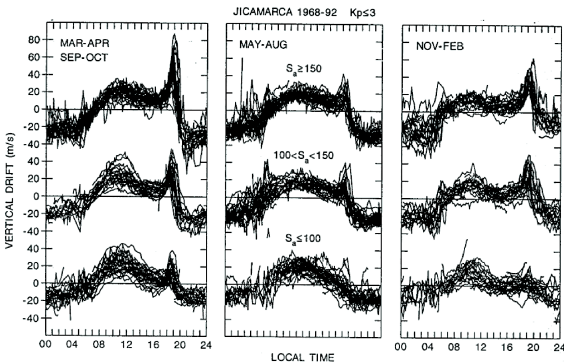
rocket measurements



vertical drifts (daytime)

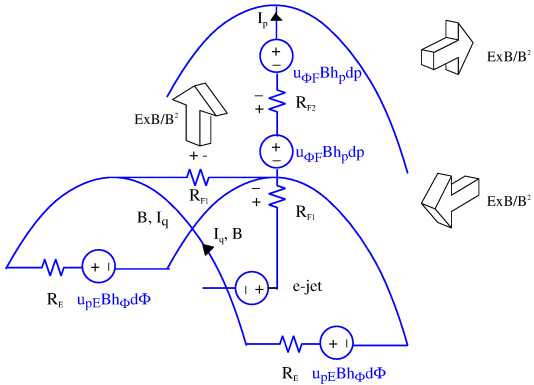


prereversal enhancement

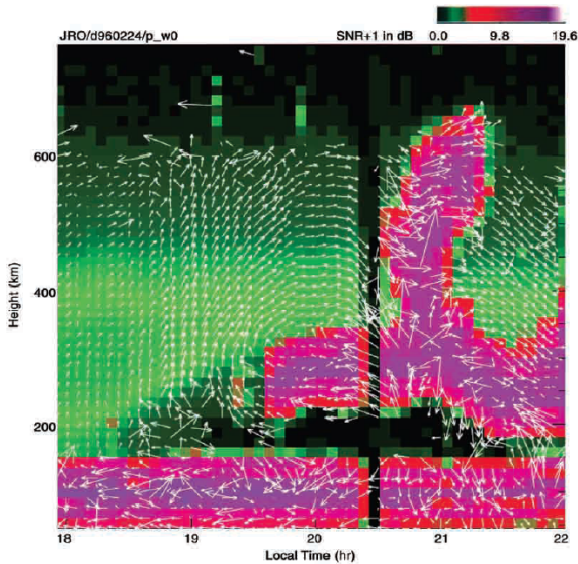


Scherliess and Fejer, *J. Geophys. Res.*, 104, 682, 1999

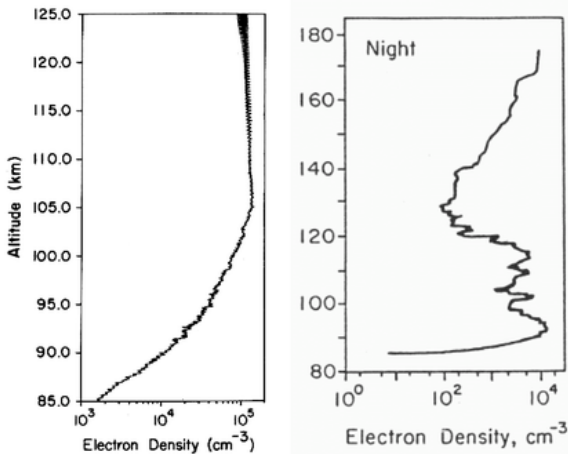
prereversal enhancement



vorticity

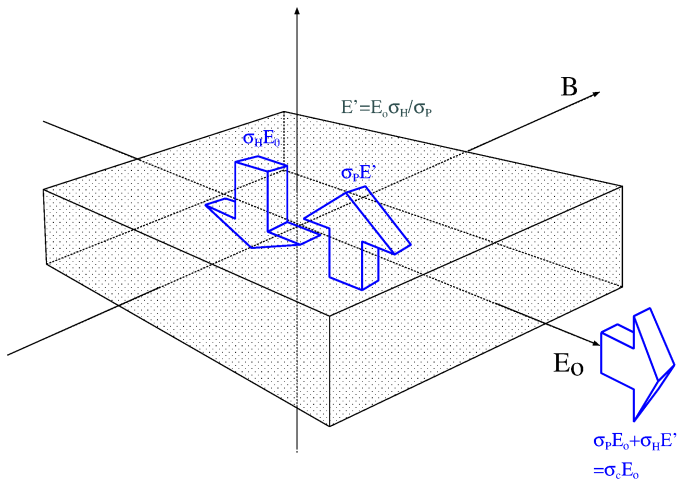


E layer



From Pfaff, *J. Atmos. Terr. Phys.*, 53, 709, 1991 and Prakash et al., *Indian J. Radio Space Phys.*, 72, 1, 1972.

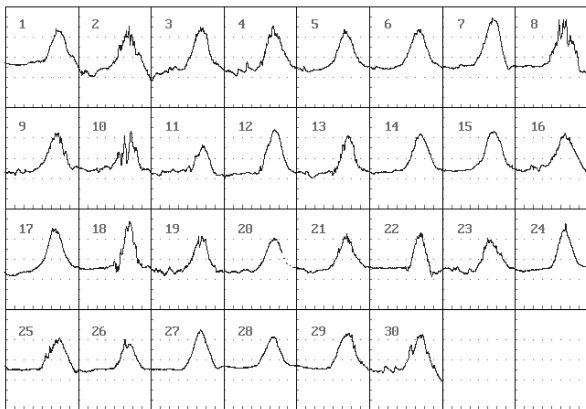
slab electrojet current model (daytime)



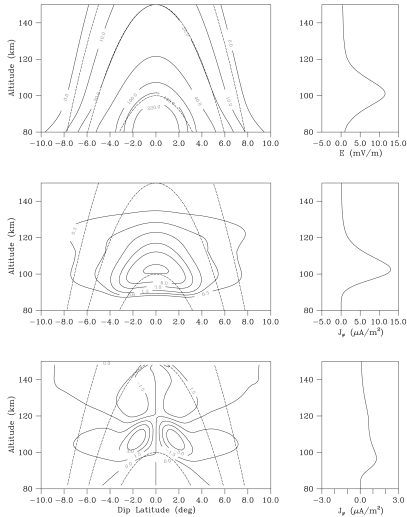
Jicamarca magnetometer

Estacion : Jicamarca - Peru
Fecha : JUNIO 2002

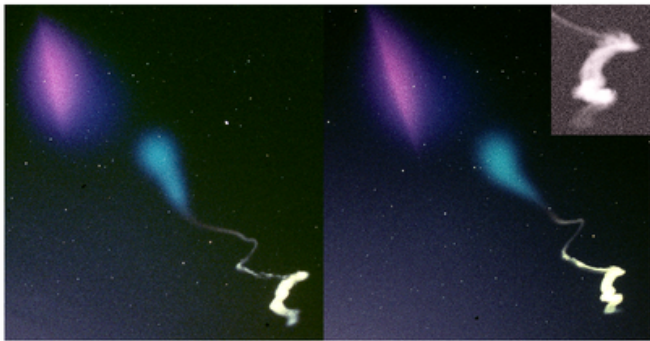
Comp. : H
Escala : 40 nT/Div



numerical model: $\nabla \cdot \mathbf{J} = 0$

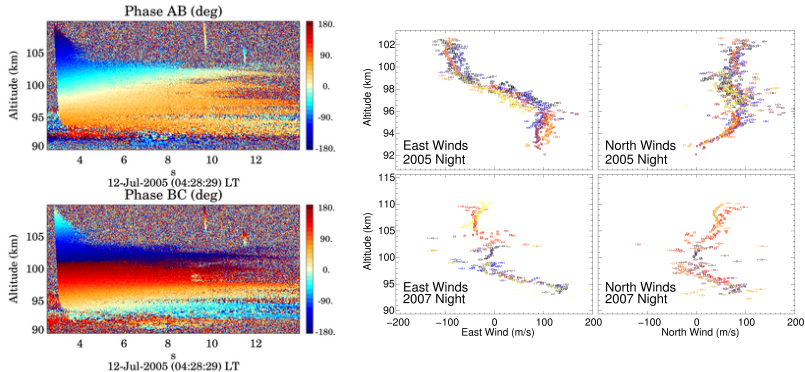


mlt winds



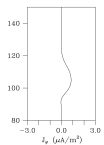
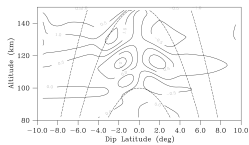
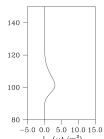
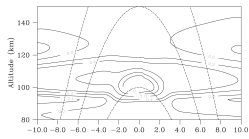
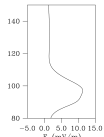
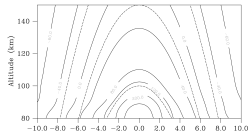
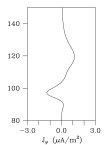
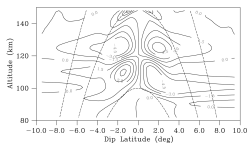
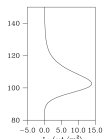
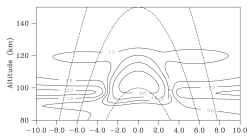
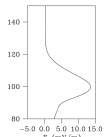
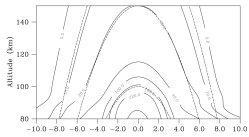
Larsen, M. F., *J. Geophys. Res.*, 107, 10.1029/2001JA000218, 2002.

meteor trail winds

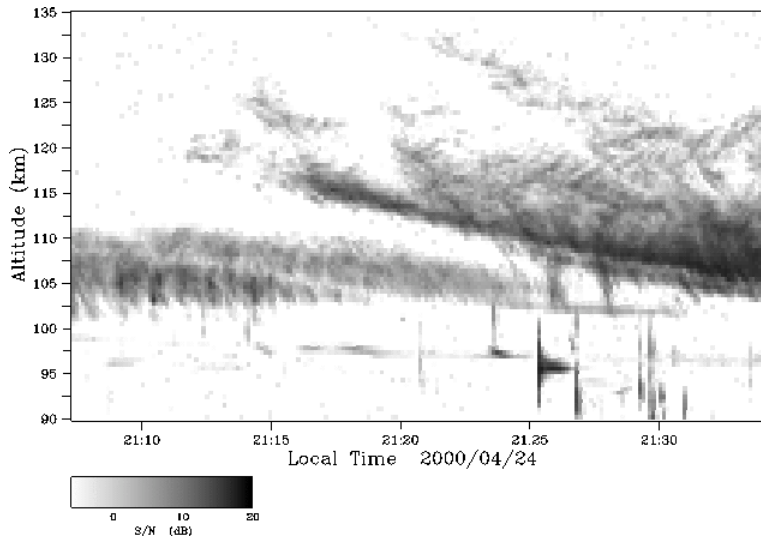


Oppenheim, M. M., et al., *Geophys. Res. Lett.*, 36, L09817, 2009

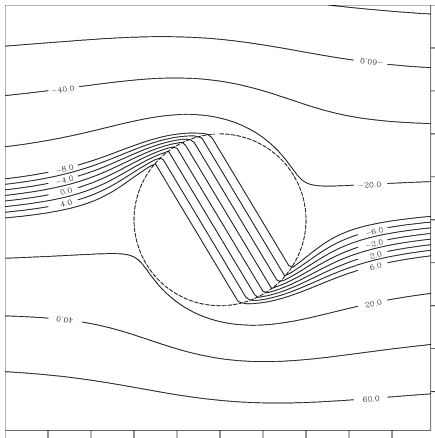
with TIME-GCM winds (noon, twilight)



electrojet plasma waves

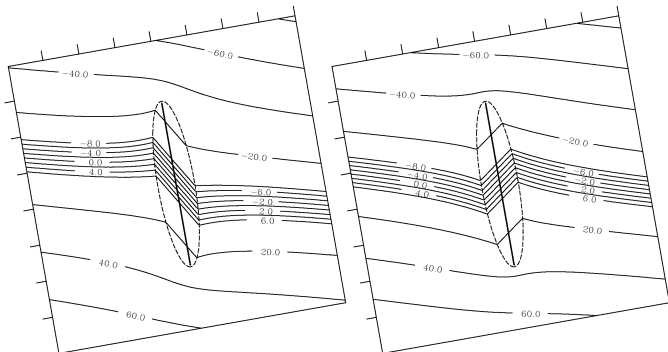


heuristic description of FBGD instability (daytime)



Solution of $\nabla \cdot \mathbf{J} = 0$ (equipotentials) for two-dimensional depletion interrupting electrojet current.

heuristic description of instability (daytime)



depletion — enhancement

FBGD: linear, local, fluid dispersion relation

$$\boxed{\frac{\partial n_j}{\partial t} + \nabla \cdot (n_j \mathbf{v}_j) = 0}$$

- seek plane wave solutions in small perturbations, linearizing and using

$$\begin{aligned}\mathbf{v}_i &= \frac{\Omega_i}{i\omega_i + \nu_{in}} \frac{\mathbf{E}_\perp}{B} - \frac{C_{si}^2}{i\omega_i + \nu_{in}} \nabla_\perp \ln n + v_{i\circ} \hat{x} \\ \mathbf{v}_e &= \frac{\mathbf{E} \times \mathbf{B}}{B^2} - \frac{\Omega_e}{\nu_{en}} \frac{\mathbf{E}_\parallel}{B} - \frac{\nu_{en}}{\Omega_e} \frac{\mathbf{E}_\perp}{B} \\ &\quad - \frac{\nu_{en}}{\Omega_e^2} C_{se}^2 \nabla_\perp \ln n - \frac{C_{se}^2}{\nu_e} \nabla_\parallel \ln n + v_{e\circ} \hat{x},\end{aligned}$$

$$C_{sj}^2 \equiv \gamma_j K_B T_j / m_j, \nu_{in} \rightarrow \nu_{in} + i\omega, \omega_i \equiv \omega - k_x v_{i\circ}, \omega_e \equiv \omega - k_x v_{e\circ} - k_x V_d,$$

FBGD: linear, local, fluid dispersion relation

ions:

$$\left(i\omega_i + \frac{C_{si}^2}{i\omega_i + \nu_{in}} k_\perp^2 \right) n_1 + n_\circ \frac{\Omega_i}{i\omega_i + \nu_{in}} k_\perp^2 \frac{1}{B} \phi_1 = 0$$

electrons:

$$\begin{aligned} & \left(i\omega_e + \frac{\nu_{en}}{\Omega_e^2} C_{se}^2 k_\perp^2 + \frac{C_{se}^2}{\nu_{en}} k_\parallel^2 \right) n_1 \\ & + \left(ik_x \frac{\partial n_\circ}{\partial z} \frac{1}{B} - n_\circ \frac{\Omega_e}{\nu_{en}} k_\parallel^2 - n_\circ \frac{\nu_e}{\Omega_e} k_\perp^2 \frac{1}{B} \right) \phi_1 = 0 \end{aligned}$$

$$\omega_r = \frac{k_x(V_d + v_{e\circ} - v_{i\circ})}{1 + \psi} + k_x v_{i\circ}$$

$$\gamma = \frac{1}{1 + \psi} \left[\frac{\psi}{\nu_{in}} (\omega_{ir}^2 - k_\perp^2 C_s^2) - \frac{\omega_{ir}}{L} \frac{k_x}{k_\perp^2} \frac{\nu_{in}}{\Omega_i} \right]$$

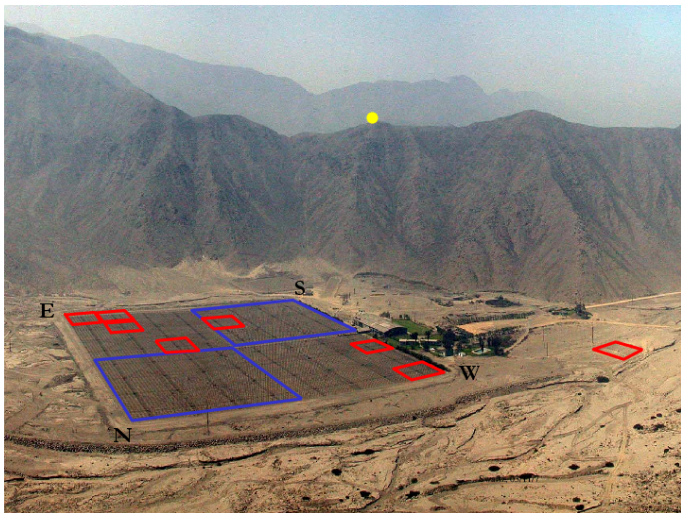
$$C_s^2 \equiv K_B(\gamma_i T_i + \gamma_e T_e)/m_i, \psi_\circ \equiv \nu_{en} \nu_{in} / \Omega_e \Omega_i, \psi \equiv \psi_\circ [1 + (\Omega_e^2 / \nu_{en}^2)(k_\parallel^2 / k_\perp^2)]$$

theory shortcomings

- Theory places peak electrojet current at 101 km altitude whereas observations indicate 106–108 km.
- Theory underestimates wavelengths of dominant gradient drift waves (particularly at night) and overestimates their phase speeds (by about a factor of 2).
- Theory predicts that Farley Buneman waves should propagate at the electron drift speed whereas experiment shows that they propagate at about the ion acoustic speed (marginal growth condition).
- Theory predicts horizontally propagating waves only whereas radar detects waves propagating at all zenith angles.

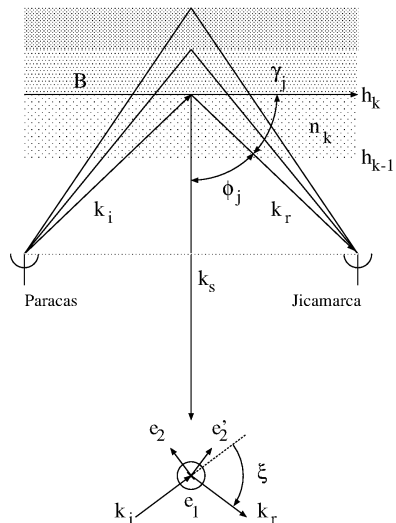
Most of the aforementioned behavior has been successfully recovered through numerical simulations incorporating nonlinear, nonlocal, and anomalous effects.

radar imagery



daytime nighttime

bistatic radar measurements

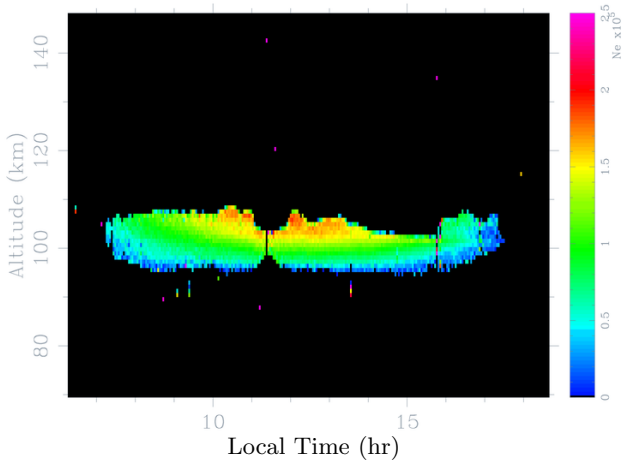


Paracas/ Jicamarca



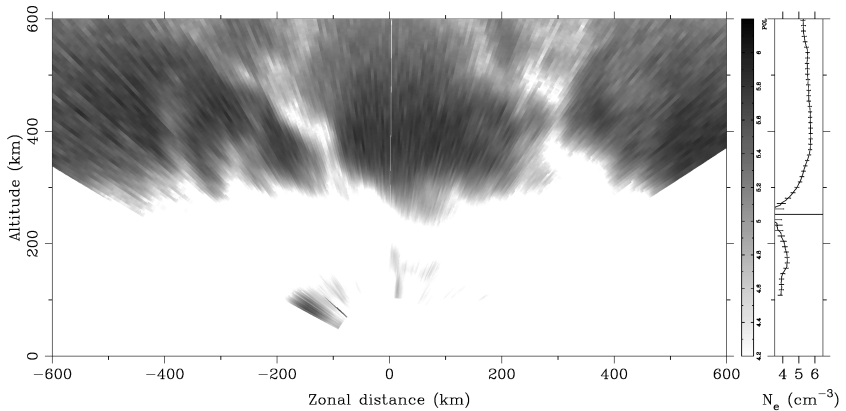
coherent scatter Faraday rotation

Fri Apr 23 18:39:52 2004

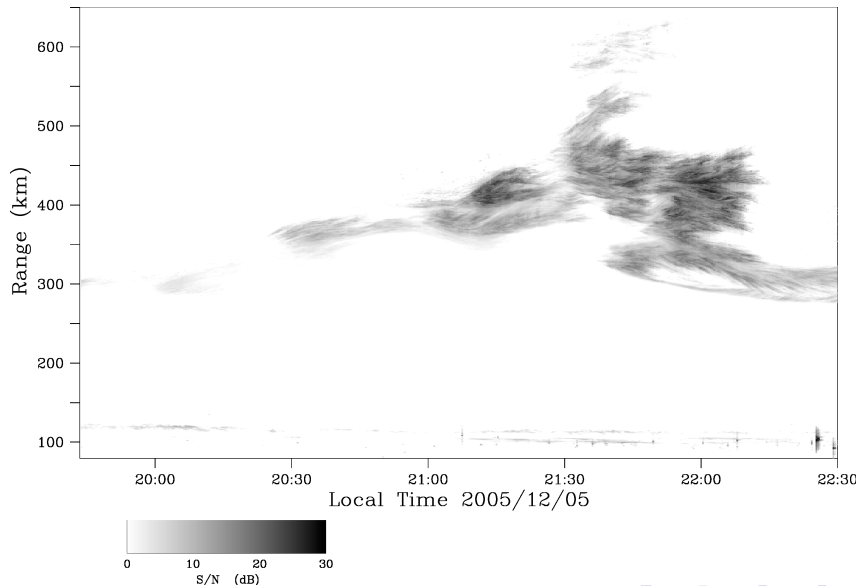


equatorial spread F

Wed Aug 11 10:09:04 2004

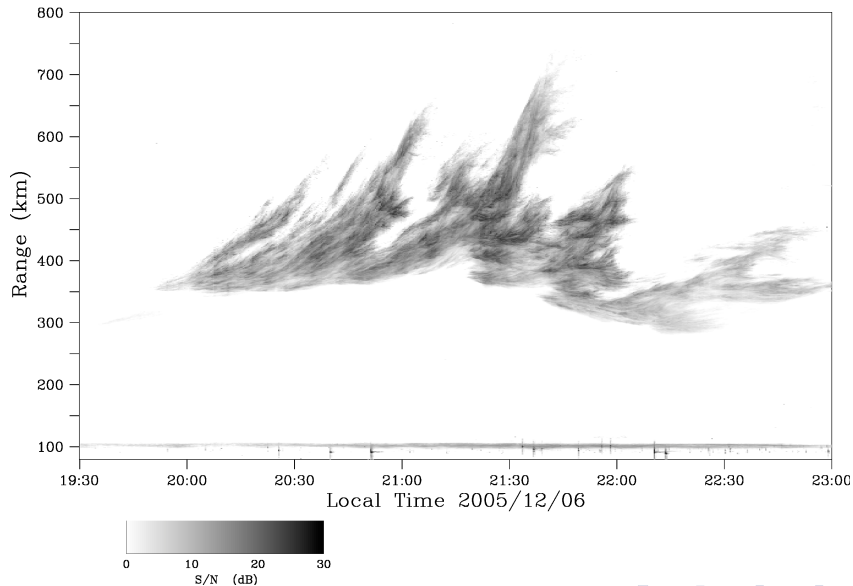


radar imagery

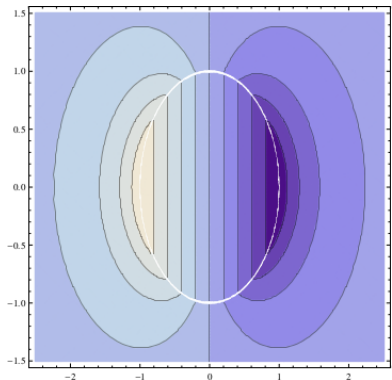


Dec 5

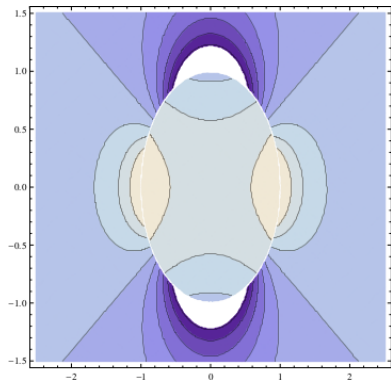
radar imagery



heuristic gRT theory: 3D warm plasmas; plan view



polarization



ambipolar diffusion

Drake, J. F., and J. D. Huba, *Phys. Rev. Lett.*, 58, 1987

linear, local theory for collisional interchange instability

$$\frac{\partial n_i}{\partial t} + \nabla \cdot (n_i \mathbf{v}_i) = 0$$

$$\gamma n_1 + \frac{1}{h_p} \frac{dn_\circ}{dp} \frac{ik_\phi}{h_\phi B} \phi_1 = 0$$

$$0 = \nabla \cdot \mathbf{J} = \frac{\partial}{\partial q} (h_p h_\phi J_q) + \frac{\partial}{\partial \phi} (h_p h_q J_\phi)$$

$$= \int_{E-E}^E dq \underbrace{\frac{\partial}{\partial \phi}}_{\leftarrow} \left[h_p h_q \frac{\sigma_P}{n_\circ} \left(n_1 \left\{ E_\phi - u_p B + \frac{g}{\nu_{in}} B \right\} + n_\circ \frac{ik_\phi}{h_\phi} \phi_1 \right) \right]$$

$$\gamma = \frac{\int dq \frac{h_p h_q}{h_\phi} \sigma_P \left(E_\phi / B - u_p + \frac{g}{\nu_{in}} \right) \frac{1}{n_\circ h_p} \frac{dn_\circ}{dp}}{\int dq \frac{h_p h_q}{h_\phi} \sigma_P}$$

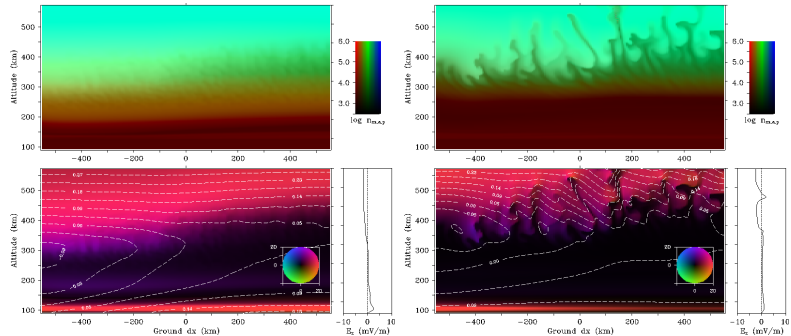
instability driven by vertical currents

Preceding analysis considered effect of zonal currents only.
Vertical currents are also destabilizing. Plane wave solutions propagating in vertical and zonal directions need to be considered.

$$\gamma = \frac{k_\Phi k_p \int dq h_q \sigma_P (u_\Phi - v_\Phi) \frac{1}{n_\circ h_p} \frac{dn_\circ}{dp}}{k_\Phi^2 \int dq \frac{h_p h_q}{h_\Phi} \sigma_P + k_p^2 \int dq \frac{h_\Phi h_q}{h_p} \sigma_P}$$

In this case, dynamo inefficiency is crucial for instability!

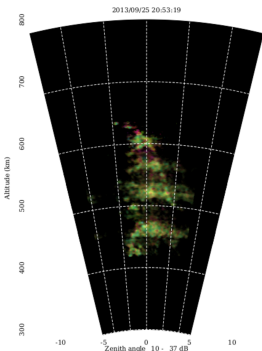
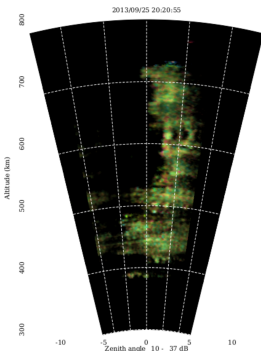
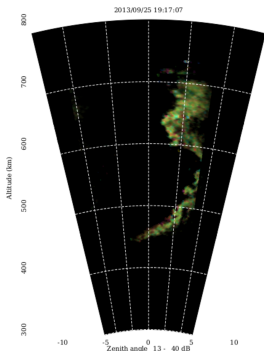
3D numerical simulation (less diamagnetic current)



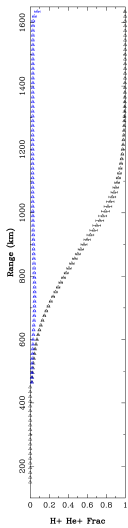
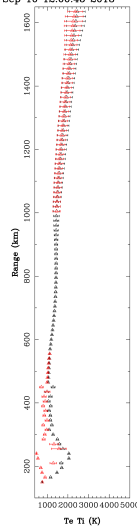
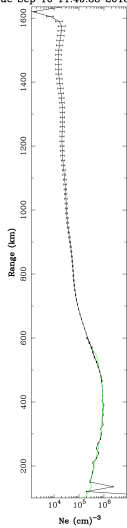
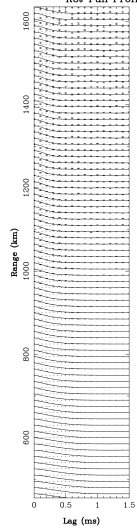
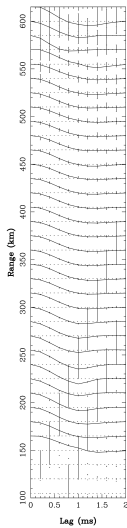
2345 UT + 25 min.

2345 UT + 75 min.

radar images – high activity



topside 12 LT



temperature and composition

- At low altitudes, composition controlled by local photochemistry, temperature controlled by local heating and cooling.
- At higher altitudes, material and heat transport (diffusion, thermal diffusion) become important. Heat budget in topside also affected by energetic electron transport.
- Main topside light-ion reactions are $H^+ - O^+$ charge exchange for hydrogen ions and photoionization/ radiative recombination for helium ions.

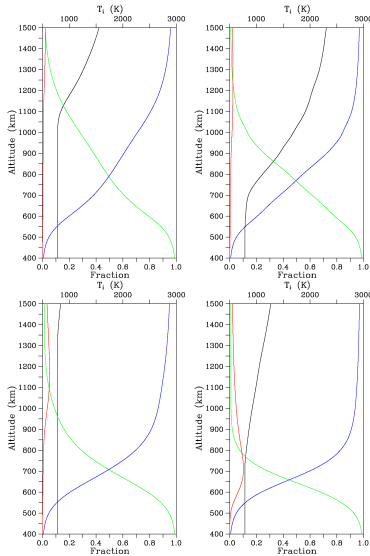
diffusive equilibrium (late afternoon)

$$\begin{aligned} 0 &= -K \nabla(n_j T)/n_j + eE - m_j g \\ 0 &= -K \nabla(n_e T)/n_e - eE \end{aligned}$$

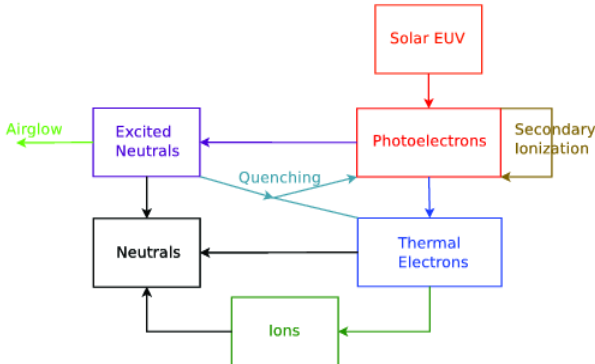
$$n_e = \sum_j n_j, \quad T_j = T_e = T$$

$$\frac{n_j(z)}{n_e(z)} = \frac{n_{oj} e^{-\int_{\odot}^z dz/H_j}}{\sum_i n_{oi} e^{-\int_{\odot}^z dz/H_i}}$$

$$H_j \equiv \frac{KT(z)}{m_j g(z)}$$



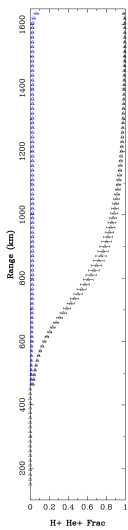
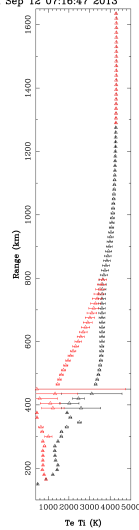
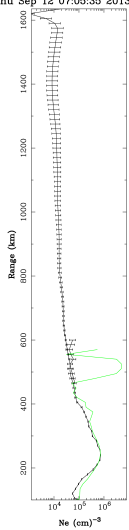
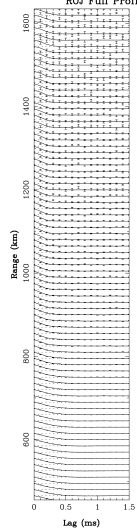
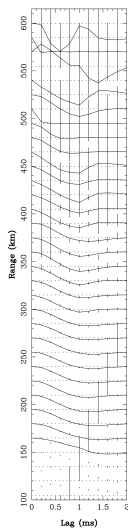
Equatorial ionosphere seldom in diffusive equilibrium!



from Varney, Cornell Univ., 2012

Photoelectrons degraded by pitch-angle scattering, elastic, and inelastic collisions as they propagate along B , preserve the 1st adiabatic invariant, undergo trapping, and ultimately return to the thermal electron population.

topside 07 LT



- Dynamics arise from wind-driven ionospheric currents, inhomogeneous, anisotropic conductivity, and the requirement of quasineutrality. Interesting flow features accompany regions with steep conductivity gradients.
- Most obvious features are the evening vortex in the *F* region and the equatorial electrojet in the *E* region.
- Plasma instabilities arise when the flow around conductivity irregularities is such as to deepen the irregularities. The main instabilities are FBGD in the *E* region and ESF in the *F* region.
- Topside composition not quite consistent with diffusive equilibrium.
- Heat flows from photoelectrons to thermal electrons to ions to neutrals. Energetic electron transport important around dawn.